Fluctuation of Surface Charge in Membrane Pores

C. Lindsay Bashford, Glenn M. Alder, and Charles A. Pasternak
Department of Biochemistry and Immunology, Cellular and Molecular Sciences Group, St George's Hospital Medical School, University of London, London SW17 0RE, United Kingdom

ABSTRACT Surface charge in track-etched polyethylene terephthalate (PET) membranes with narrow pores has been probed with a fluorescent cationic dye (3,3′-diethyloxacarbocyanine iodide (diO-C_2-(3))) using confocal microscopy. Staining of negatively charged PET membranes with diO-C_2-(3) is a useful measure of surface charge for the following reasons: 1) the dye inhibits K^+ currents through the pores and reduces their selectivity for cations; 2) it inhibits [^{3}H]-choline$^+$ transport and promotes $^{36}Cl^-$ transport across the membrane in a pH- and ionic-strength-dependent fashion; and 3) staining of pores by diO-C_2-(3) is reduced by low pH and by the presence of divalent cations such as Ca^{2+} and Zn^{2+}. Measurement of the time dependence of cyanine staining of pores shows fluctuations of fluorescence intensity that occur on the same time scale as do fluctuations of ionic current in such pores. These data support our earlier proposal that fluctuations in ionic current across pores in synthetic and biological membranes reflect fluctuations in the surface charge of the pore walls in addition to molecular changes in pore proteins.

INTRODUCTION

Certain properties of solutions, such as viscosity (Granick, 1991; Bhushan et al., 1995), with the exception of water (Raviv et al., 2001), and ion conductance (Schwartz, 1962; Lakshminarayanaiah, 1969; Manning, 1969), deviate from the value in bulk solution when measured near a surface. In the case of ion conductance, an abnormally high value in a region that is within a Debye length or so of a charged surface, termed surface conductance, has been ascribed to an accumulation of counterions (Spitzer, 1984). We have suggested that fluctuation of conductance in synthetic membrane pores (Lev et al., 1993) and other materials (Sachs and Qin, 1993) in which surface conductance contributes significantly to total conductance, is due to oscillation in the concentration of counterions along the surface of the pore (Korchev et al., 1997) and that this results from a fluctuation in surface charge. Here we document this effect.

Track-etched polyethylene terephthalate (PET) membranes bear fixed negative charges at their surface and within pores, due to the free carboxyl groups that are generated by alkaline hydrolysis of ester bonds during the etching process. We have calculated that there are ~1.6 such ionizable groups per nm^2 of PET (Korchev et al., 1997); this density happens to approximate the number of charged groups at the surface of a phospholipid bilayer. Such charges attract positively charged counterions from solutions in which the membrane is bathed. As a result, the conductance through narrow pores in which the surface area of the pore is large in comparison with its volume, is anomalously high (Korchev et al., 1997). That is, the conductance is made up of two quantities: the conductance of the bulk solution plus the surface conductance. With 2–3-nm-diameter pores and solutions of low ionic strength (<0.5 M) at pH 7, surface conductance exceeds bulk conductance by more than 100-fold (Lev et al., 1993); under these conditions the transference number $t_+ > 0.9$ and the pore is cation selective (Lev et al., 1993). In wider pores, bulk conductance swamps surface conductance, which then contributes relatively little to total conductance, so that t_+ approaches 0.5 (equal contribution to current by cations and anions). Although we accept that there is no theoretical relationship between conductance and selectivity, or between conductance and permeability for that matter, our results show that in PET membranes conductance and selectivity (Korchev et al., 1997), as well as conductance and permeability (Rostovtseva et al., 1996), do alter in concert. A diminution of surface conductance relative to bulk conductance is also seen in narrow pores at high ionic strength, at which the accumulation of counterions by the fixed negative charges of the PET membrane is saturated, or screened. Surface conductance in narrow pores is depressed also at low pH due to protonation of the carboxyl groups, by methylation of carboxyl groups (Pasternak et al., 1995), and by the presence of divalent cations that bind to carboxyl groups (Lev et al., 1993). Here we demonstrate that the binding of a counterion, namely, the charged dye 3,3′-diethyloxacarbocyanine iodide, indeed fluctuates in a narrow PET pore. This effect, in addition to that due to molecular changes in protein architecture, needs to be taken into account when defining the origin of fluctuations in endogenous ion channels and in pores induced across the plasma membrane of susceptible cells by bacterial toxins (Bashford and Pasternak, 2000).

Submitted October 30, 2000, and accepted for publication January 25, 2002.

Address reprint requests to Dr. C. L. Bashford, Department of Biochemistry and Immunology, Cellular and Molecular Sciences Group, St George's Hospital Medical School, London SW17 0RE, UK. Tel.: 44-020-8725-5770; Fax: 44-020-8725-2992; E-mail: l.bashford@sghms.ac.uk.

0006-3495/02/04/2032/09 $2.00

MATERIALS AND METHODS

Sheets of PET membranes were exposed to a beam of high-energy nuclei applied at right angles to create tracks through the material, which is then

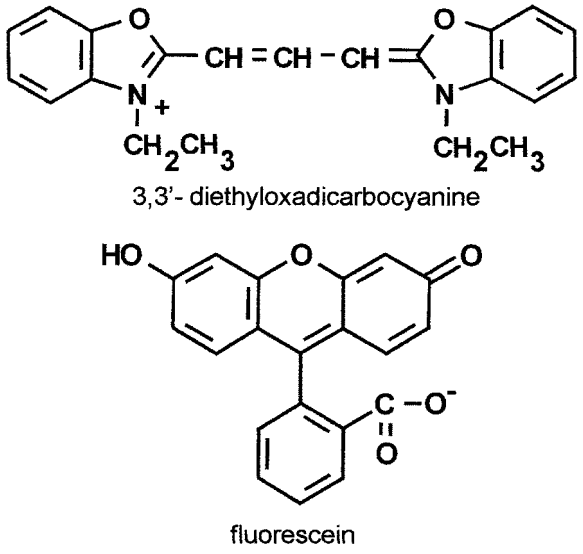

FIGURE 1 Structural formulas of 3,3′-diethyloxacarbocyanine (diO-C_2-(3)) and fluorescein.

etched in warm alkali to expand tracks into pores (Spohr, 1990). The material we used was ~10 μm thick and had a pore density of 1.1×10^6 cm^{-2}. This was measured by exposing one of many membranes being irradiated simultaneously to a long period of etching, so that pores become large enough to be visible by negative-stain electron microscopy and can therefore be counted. The pores had a nominal diameter of 20 nm as measured by gas diffusion across dry membranes (P.Y. Apel, Joint Institute for Nuclear Research, Dubna, Russia, 1993, personal communication), but as assessed in the wet state by the diffusion of small molecules and ions (Rostovtseva et al., 1996) the average effective diameter was 2–3 nm. The cyanine dye diO-C_2-(3) (Fig. 1) (Sims et al., 1974) was obtained from Molecular Probes (Eugene, OR); fluorescein (Fig. 1) was from BDH (Poole, U.K.).

To measure ion currents and ion selectivity PET membranes were clamped across the orifice (diameter ≈ 0.5 cm) between two Teflon chambers using high-vacuum silicone grease to prevent leakage. Solutions containing KCl and potassium phosphate buffers without or with diO-C_2-(3) were added to each chamber, and ion current and ion selectivity were determined via Ag/AgCl electrodes (Lev et al., 1993). Reversal potentials were recorded directly by operating the apparatus in (zero) current-clamp rather than voltage-clamp mode. We used a fast integrative capacitor in the feedback loop (Korchev et al., 1997); the output voltage of the integrator was used to control the membrane potential via virtual ground of the head amplifier to keep zero current through the membrane and to monitor the reversal potential continuously.

To measure the flow of radioactive ions across PET, the membrane was placed in a flow dialysis chamber (Rostovtseva et al., 1996). The upper chamber, which was stirred continuously, contained 0.5 ml of the solution containing radioactive ions; an identical solution without radioactivity was pumped through the lower chamber at a constant rate (~0.25 ml/min) and collected as 0.5-ml fractions. The area of the membrane in contact with the solution in both chambers was 0.5 cm^2. Radioactivity was assessed in each fraction by liquid scintillation counting. Radioactivity in the upper solution was sampled from time to time by removing 5-μl samples for liquid scintillation counting.

For confocal microscopy, small pieces of PET were immersed for 5 min in phosphate- or Hepes-buffered solutions containing dye (~5 μg/ml) and adjusted to the requisite pH, placed on a glass slide, and sealed beneath a coverslip with nail varnish. A Zeiss LSM 410 Invert confocal microscope was used to examine the samples with a laser beam transmitting at 488 nm and recording fluorescence above 515 nm. Samples were first scanned in the *xy* plane to locate suitably stained pores for study. A scan in the *z* plane was performed to check the penetration of pores by dye. An area in the *xy* plane of 8×400 pixels was then chosen and exposed to a sequence of 30 or 50 laser pulses of ~1 s duration at 3-s intervals. The resulting images at a point half way through the membrane were analyzed in a time sequence as shown in the figures. Fluorescence intensity of individual pores during the time sequence in the same optical section was tabulated and their correlation coefficient computed by standard methods (Excel 97). Flare from staining at either surface (in the case of diO-C_2-(3)) or from the solution (in the case of fluorescein) prevented analysis of images at the surface of the membrane.

RESULTS

To validate the assumption that binding to PET membranes of the cationic dye diO-C_2-(3) mimics the attraction of inorganic and other organic cations, we have examined the effect of the dye on the anomalously high flow of cations through narrow pores. First, we show that diO-C_2-(3) indeed competes with K^+ in so far as it reduces ion current (Fig. 2 *a*) and ion selectivity (Fig. 2 *b*). Both results are compatible with the suggestion that dye binds to negatively-charged sites on the membrane, to which K^+ is attracted. Another way to measure ion flow through PET membranes is to assess the rate of equilibration of radioactive ions across the membrane by the flow dialysis technique (Rostovtseva et al., 1996). Fig. 3 (*panel i*) shows that the flow of [^{3}H]choline$^+$ is inhibited by diO-C_2-(3) whereas that of $^{36}Cl^-$, which is more than sixfold slower as anticipated from selectivity measurements (Fig. 2 *b*), is slightly increased. Raising ionic strength would be expected to negate this effect (Lev et al., 1993), which is what is observed (Fig. 3, *panel ii*; note that in this panel the ratio of ^{3}H to ^{36}Cl is plotted, to show the effect more clearly). We conclude that diO-C_2-(3) is a useful cation with which to probe the movements of water-soluble ions.

We next investigated the binding of diO-C_2-(3) by direct measurement of its fluorescence. The experiments were carried out at different pH values and in the presence of divalent cations, as these parameters are known to affect ion flow (Lev et al., 1993). The results are illustrated in Fig. 4, *a–e*. The horizontal bands at the top and bottom of each picture reflect the binding of the dye to the two surfaces of the membrane; their width is due to the flare of the fluorescence at high dye concentration. Staining is more intense at pH 11 (Fig. 4 *a*) than at pH 5 (Fig. 4 *b*) (the fluorescence of diO-C_2-(3) itself is unaffected by pH). Staining within the membrane occurs only in certain regions, which are interpreted to indicate the presence of pores; similar results are obtained with negative-stain electron microscopy. The solution (the gap between the membrane and the coverslip) is seen to be unstained, but the dye binds to the coverslip (topmost part of Fig. 4 *b*) in addition to both membrane surfaces. As anticipated, divalent cations reduce the intensity of bound dye at the surface and within pores (Fig. 4, *c–e*: *c*, control; *d*, 0.1 mM $ZnSO_4$; *e*, 5 mM $CaCl_2$). Note

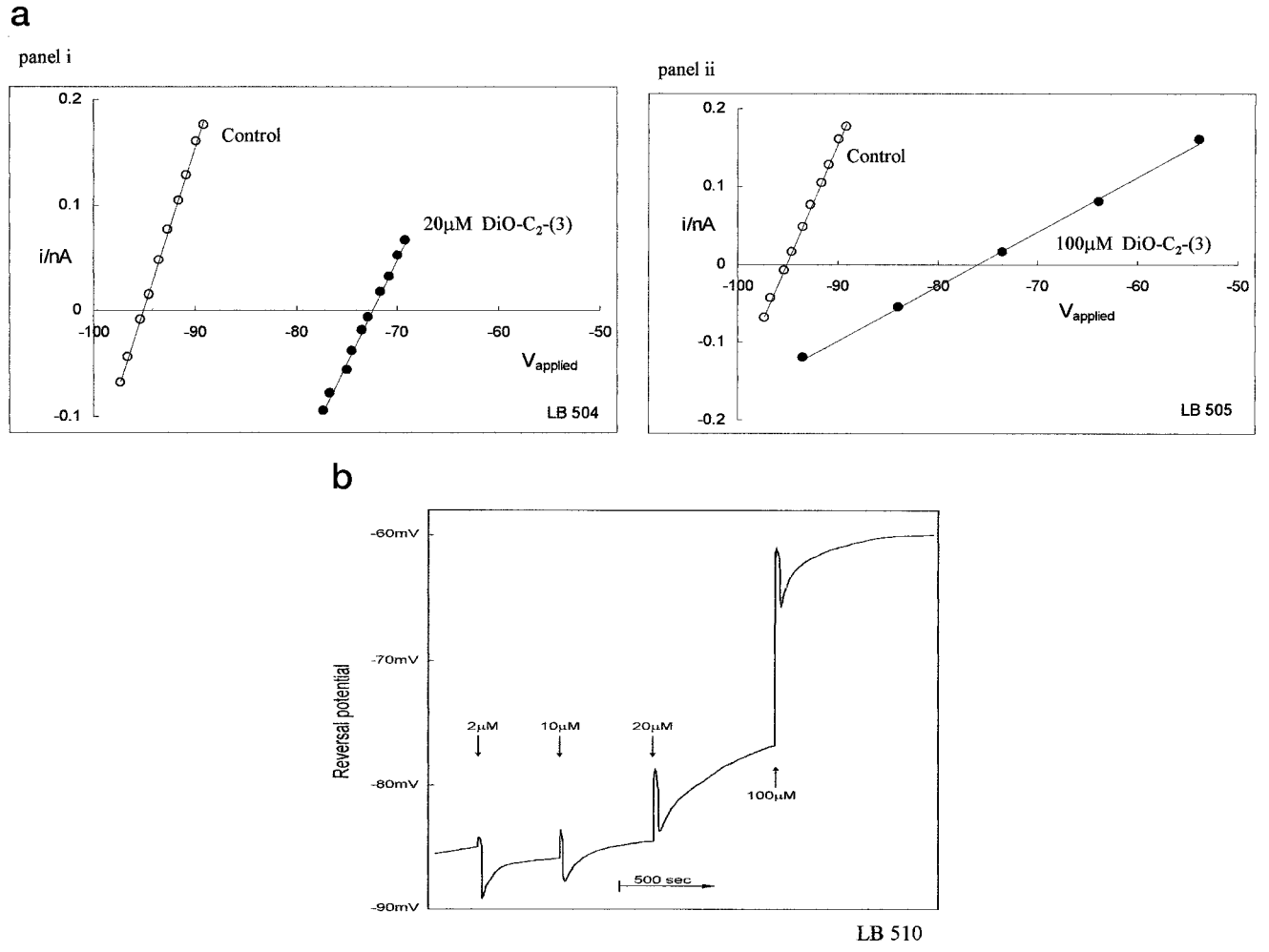

FIGURE 2 Effect of diO-C_2-(3) on ion currents and reversal potential in track-etched PET membranes. (*a*) The PET membrane contained 1.1×10^6 pores/cm^2; nominal pore diameter was 0.02 μm. $V_{applied}$ refers to the virtual ground side of the chamber, which contained 0.01 M KCl and 0.001 M K_3PO_4, pH 10.4. The other chamber contained 0.1 M KCl and 0.001 M K_3PO_4, pH 10.4, without or with 20 μM diO-C_2-(3) (*panel i*) or with 100 μM diO-C_2-(3) (*panel ii*). (*b*) The PET membrane contained 3×10^8 pores/cm^2; nominal pore diameter was 0.02 μm. Reversal potential was monitored with the virtual ground side of the chamber containing 0.01 M KCl and 0.001 M K_3PO_4, pH 10.4, and the other chamber, to which diO-C_2-(3) was added to give the final concentration indicated, containing 0.1 M KCl and 0.001 M K_3PO_4, pH 10.4.

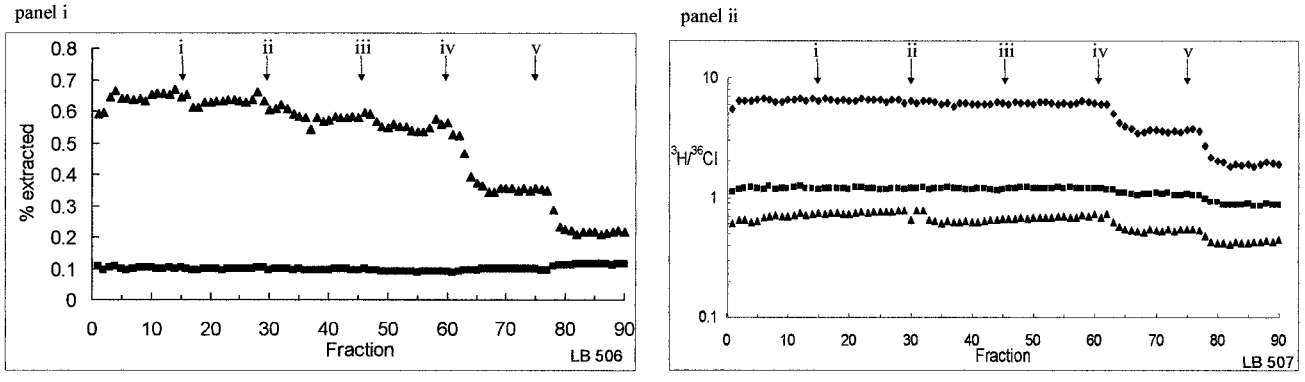

FIGURE 3 Effect of diO-C_2-(3) on ion fluxes across a track-etched PET membrane. The PET membrane contained 3×10^8 pores/cm^2; nominal pore diameter was 0.02 μm. (*Panel i*) The medium contained 0.01 M choline chloride, 0.001 M K_3PO_4, pH 10.4. [^{3}H]choline (▲) and $^{36}Cl^-$ (■) were added to the upper chamber and flow dialysis (2 min per fraction) performed without or with 2 μM (*i*), 10 μM (*ii*), 30 μM (*iv*), and 110 μM (*v*) diO-C_2-(3); or DMSO (*iii*). (*Panel ii*) The medium contained 0.01 M (♦) or 0.1 M (■) choline chloride, 0.001 M K_3PO_4, pH 10.4; or 0.01 M (▲) choline chloride, 0.001 M KH_2PO_4, pH 4.5. [^{3}H]choline and $^{36}Cl^-$ were added to the upper chamber and flow dialysis (2 min per fraction) performed without or with 2 μM (*i*), 10 μM (*ii*), 30 μM (*iv*), and 110 μM (*v*) diO-C_2-(3); or DMSO (*iii*).

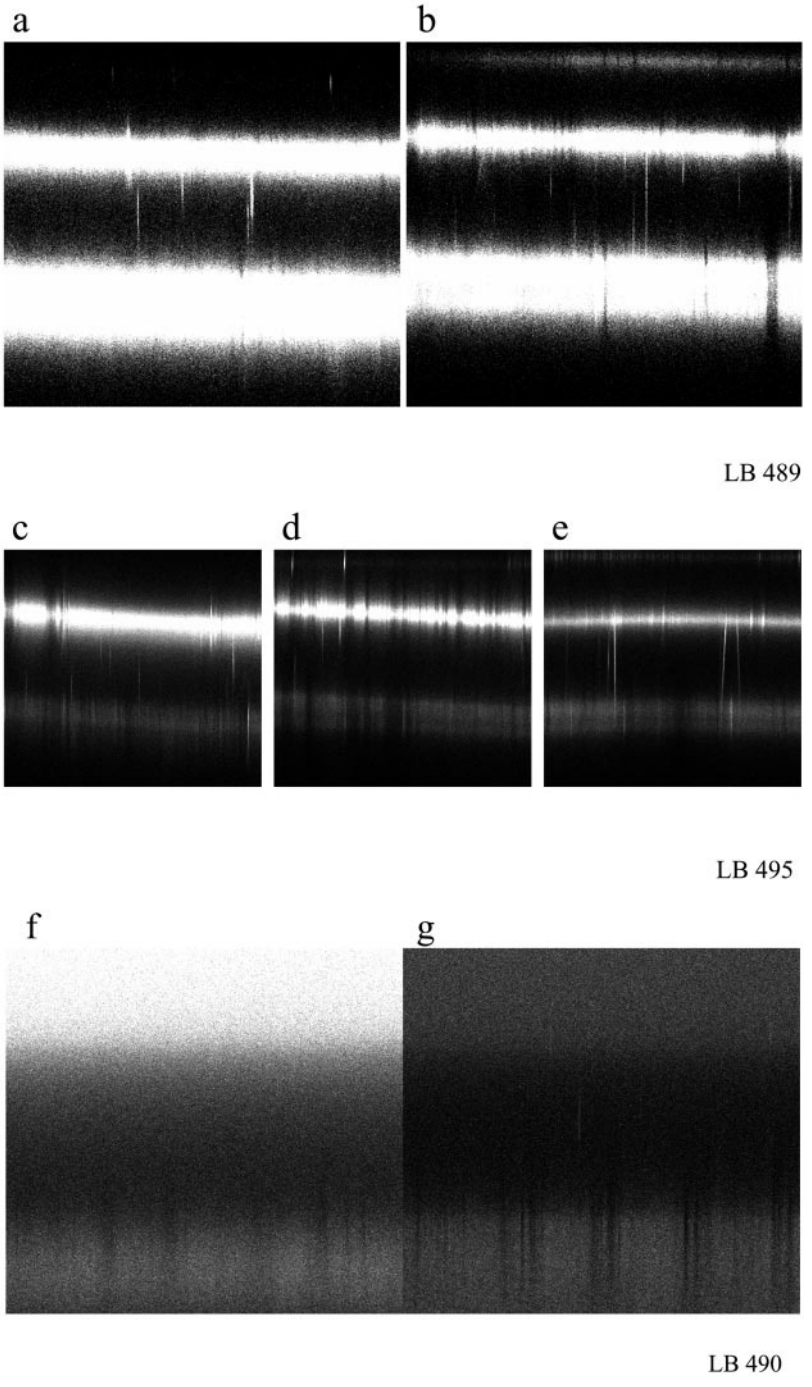

FIGURE 4 DiO-C_2-(3) and fluorescein staining of PET membrane pores. PET membranes containing 1.1×10^6 pores/cm^2 with diameters of ~20 nm were bathed in the following solutions with 10^{-6} M diO-C_2-(3): 0.1 M K_3PO_4, pH 11 (*a*); 0.1 M KH_2PO_4, pH 4 (*b*); 0.1 M KCl, 0.005 M Hepes, pH 7.4 without (*c*) or with 10^{-4} M $ZnSO_4$ (*d*) or 0.005 M $CaCl_2$ (*e*). The same membranes were bathed in the following solutions with 5 μg/ml fluorescein in 1 M KCl: 0.01 M K_3PO_4, pH 11 (*f*); 0.01 M KH_2PO_4, pH 4 (*g*). Images were obtained with a Zeiss LSM 410 invert confocal microscope using a ×63/1.4(NA) oil-immersion objective; fluorescence above 510 nm was excited at 488 nm.

that the width of bound dye at the surface, due to flare from a high concentration of dye, is decreased by divalent cations. The dimmer staining and broadening of the lower membrane/solute interface relative to the upper interface is due, in part, to an optical effect (spherical aberration) arising from the greater separation of the objective lens from the lower interface. The results of Fig. 4 precisely mimic the effects of pH and divalent cations on surface conductance and give us confidence that the fluorescence of diO-C_2-(3) is indeed a measure of surface charge. It is reinforced by the fact that staining with a negatively charged dye like fluorescein gives a pattern that is the opposite of that generated by diO-C_2-(3): there is intense staining of the solution but little of the membrane; few pores are visible (Fig. 4, *f* and *g*). At pH 11 (Fig. 4 *f*), staining of both solution and membrane is more intense than at pH 5 (Fig. 4 *g*) because the fluorescence of fluorescein itself is reduced at low pH.

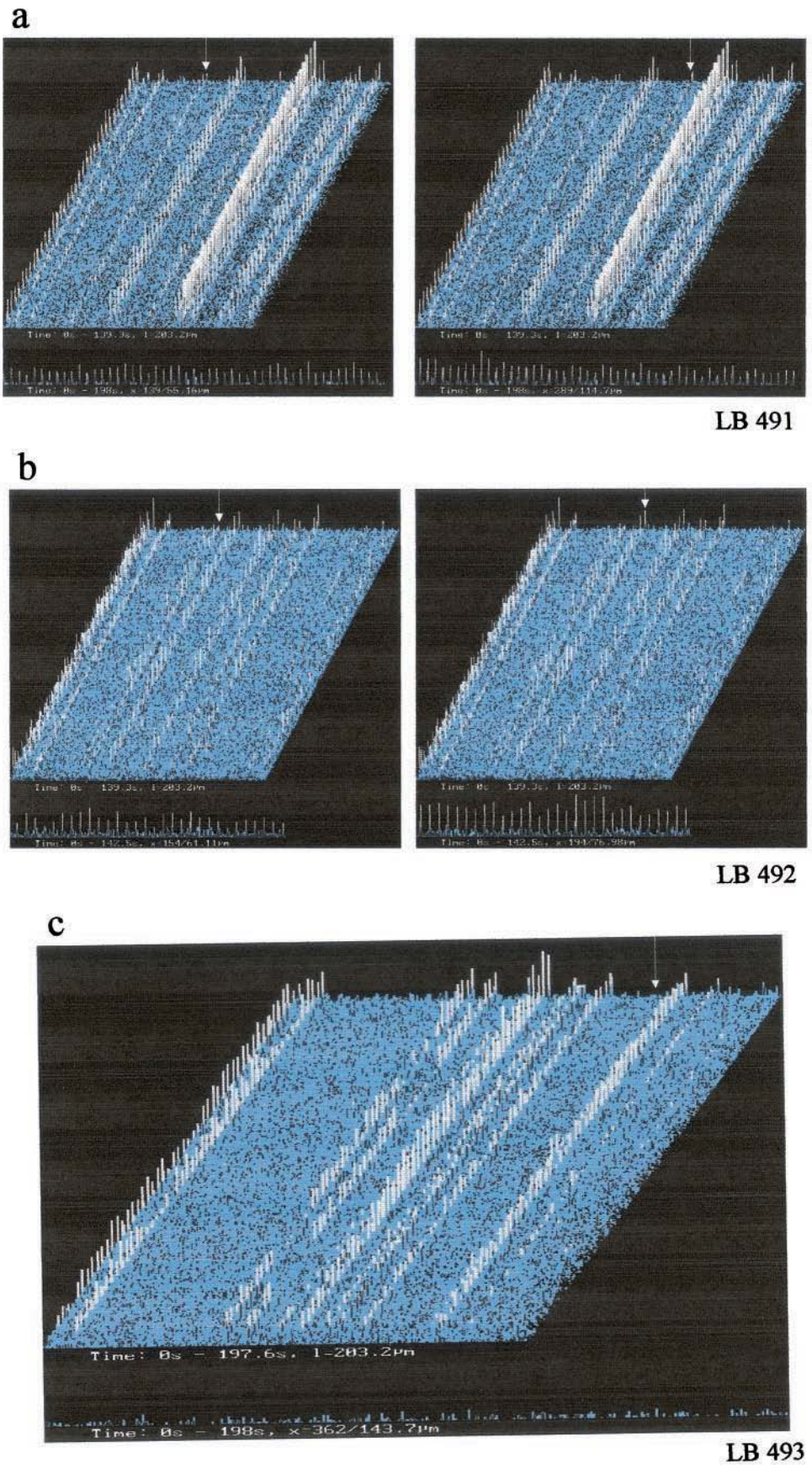
a
LB 491
b
LB 492
c
Time: 0s - 197.6s, 1-203.2μm
Time: 0s - 198s, x-362/143.7μm
LB 493

FIGURE 5(a–c)

TABLE 1 Correlation of fluctuations between adjacent pores

Correlation coefficient	Frequency
−0.5	0
−0.4	1
−0.3	0
−0.2	8
−0.1	7
0	10
0.1	9
0.2	10
0.3	7
0.4	6
0.5	0

A total of 46 pores from five different PET membranes stained with diO-C_2-(3) at various values of pH with or without $ZnCl_2$ were analyzed. The magnitude of the correlation coefficients of all possible pairs of pores in the same optical sample are presented. The two-sided 5% point for the correlation coefficient with 30 observations is 0.36, and the 1% point is 0.46 (Bland, 2000).

The effect of a timed sequence of laser pulses using diO-C_2-(3) is illustrated in Fig. 5, *a–c*. The upper part of each panel shows the fluorescence when a narrow strip of membrane in the *xy* plane is illuminated every 3 s. The height of each peak corresponds to the fluorescence intensity half way through the membrane in the *z* plane. Successive peaks, from top to bottom, show the fluorescence at the end of each laser pulse. The first thing to notice is that there is a clear difference between the fluorescence along a row of peaks, corresponding to pores, and the background fluorescence across the rest of the membrane, due to white noise. The second point is that fluorescence does not decrease with time (i.e., from top to bottom), indicating the absence of photobleaching. The third point is that the height of successive peaks is random. Finally, adjacent rows of peaks, in other words, adjacent pores, do not fluctuate in concert. The correlations between 46 different pores stained with diO-C_2-(3) under a variety of conditions is presented in Table 1. Of the 58 correlations, three showed significance at the 5% level (correlation coefficient > 0.36 or < -0.36 for 30 observations) and none showed significance at the 1% level (correlation coefficient > 0.46 or < -0.46 for 30 observations). Taken together, these results make it unlikely that fluctuations arise because of some artifact of the system. When the fluctuations of a single pore are displayed as a time sequence (lower part of each panel, from left to right), the similarity with time sequences of current fluctuations (e.g., Lev et al., 1993; Sachs and Qin, 1993; Korchev et al., 1997) is apparent.

A similar series of laser pulses, using fluorescein instead of diO-C_2-(3), is shown in Fig. 5 *d*. As might be anticipated

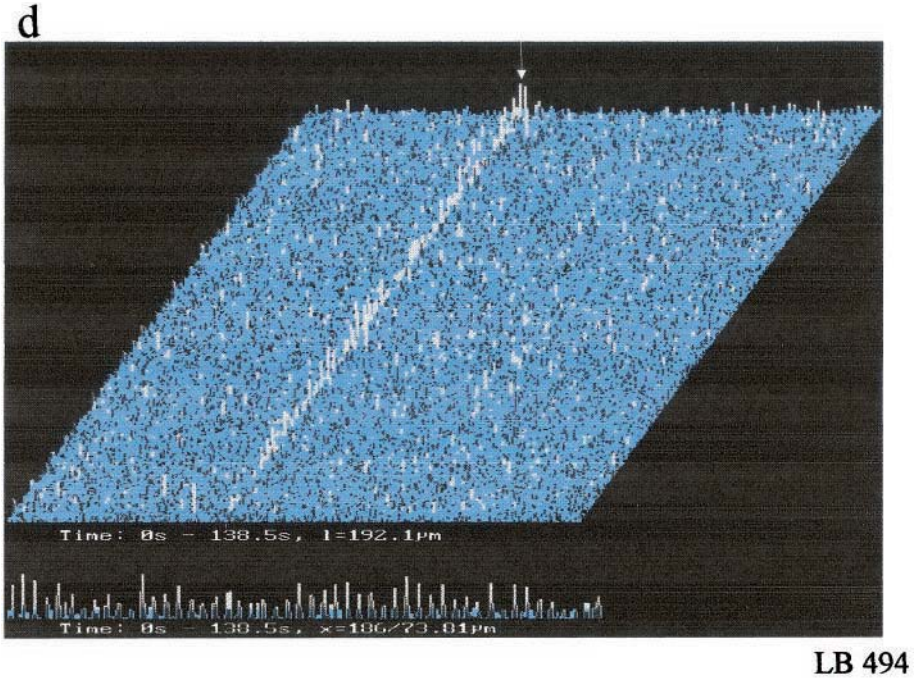

FIGURE 5 Fluctuations in DiO-C_2-(3) or fluorescein-stained PET membrane pores. PET membranes containing 1.1×10^6 pores/cm^2 with diameters of ~20 nm were bathed with 10^{-6} M diO-C_2-(3) in the following solutions: 0.1 M KH_2PO_4, pH 4 (*a*); 0.1 M K_2HPO_4, pH 8 (*b*); or 0.1 M K_3PO_4, pH 11 (*c*). The same membranes were bathed with 5 μg/ml fluorescein in 0.1 M KH_2PO_4, pH 4 (*d*). Images were obtained with a Zeiss LSM 410 invert confocal microscope using a ×63/1.4(NA) oil-immersion objective; fluorescence above 510 nm was excited at 488 nm. A box 400 pixels in the *x*-direction and 8 pixels in the *y*-direction was scanned 50 times at 3-s intervals. The images are presented as a stack with the first time point at the top of the page. The lower trace shows a time line at the *x*-pixel indicated by the white arrow at the top of the page; in *c* this image corresponds to a region where there is no pore. Both the upper image and the lower trace corresponding to one of the pores are shown as white signal superimposed on arbitrarily chosen blue background.

from the result of Fig. 4, *f* and *g*, only a few pores can be distinguished above the background noise, which indicates that most pores exclude the negatively charged dye. What pores are visible fluctuate in intensity, like the pores depicted in Fig. 5, *a–c*.

DISCUSSION

We interpret fluctuations of fluorescence to be a consequence of protonation-deprotonation of carboxyl groups within the pore; it is to the ionized form that cations are attracted. With diO-C_2-(3), increase of fluorescence reflects entry of dye due to increase of ionization (deprotonation); with fluorescein, increase of fluorescence also reflects entry of dye, in this instance due to a decrease of ionization (protonation). We conclude that fluctuations in the fluorescence of diO-C_2-(3) and of fluorescein in PET membrane pores reflect the same ionic changes that give rise to fluctuations of cation current and anion current when a voltage is applied across a PET membrane pore.

We believe that the fluctuations in fluorescence intensity we observe in PET pores arise from time-varying fluctuations in surface charge within the pore for the following reasons.

First, there are many more surface-charge-attracted dye molecules than there are free dye molecules in the pore lumen. Under the conditions of these experiments a 10-μm-long pore with a radius of 3 nm (as determined by permeation of water; Rostovtseva et al., 1996) will contain, on average, two free diO-C_2-(3) molecules (assuming that the dye concentration in the pore is 10^{-5} M, as it is in solution), and 3×10^5 negative surface charges assuming that there are 1.7 charges/nm^2 (Wolf et al., 1995). We note that free solution between the membrane and coverslip has no detectable fluorescence and conclude that the fluorescence signal we observe arises from dye molecules attracted by negative surface charges. If the confocal microscope samples 10% of the pore length (i.e., a 1-μm slice), then that slice will contain 3×10^4 surface charges. If the dye occupies 3% or more of those charged sites, then there will be at least 1000 dye molecules to be detected; with a fluorescence lifetime of 1–10 ns and a measurement time of about a second, this equates to 10^{11}-10^{12} photons.

Second, diffusion is fast enough for dye molecules to enter and leave the pores on the time scale of our fluorescence measurements, ~3 s between each line scan. If we combine Ohm's law and Fick's law to estimate flux across small pores as employed by Hille (1992) and assume that cyanine is present at 10^{-5} M and has a diffusion coefficient of $\sim 10^{-5}$ cm^2/s, then ~100,000 dye molecules/s will arrive at the mouth of a pore of radius 3 nm. If the pore is 10 μm long, the rate of diffusion of a 10^{-5} M dye solution through it is ~2000 molecules/s.

Third, the fluctuations represent a real signal, not noise due to the size of the pore or the nature of the fluorescence detection system. A priori the fluctuations we observe may represent variability of the sample or variability of the detection system, or both. We note that the day-to-day variability of fluorescence intensity of standard objects (e.g., fluorescent beads) is less than 5% and often less than 1%. We have analyzed the statistical variation of fluores-

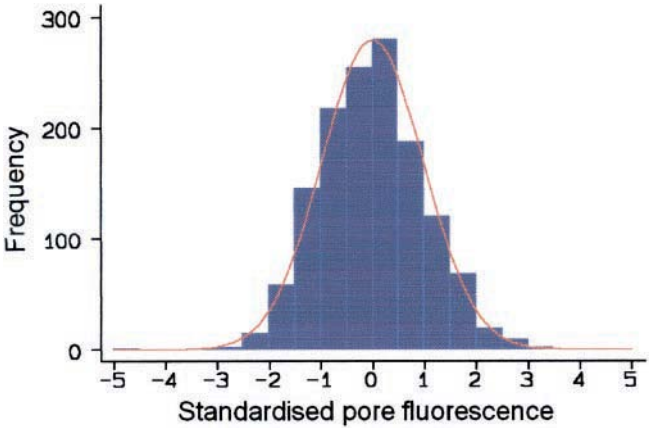

FIGURE 6 Distribution of fluorescence intensities among different PET pores exposed to DiO-C_2-(3). If we have many observations from a Poisson variable, here 30 successive determinations of fluorescence intensity in 46 different PET pores, their square root should follow a normal distribution. This will also be true if the Poisson variable is multiplied by a constant. First we took the square root of the observations of fluorescence intensity. Then for each pore separately we found the mean and standard deviation of the square root transformed data. We then subtracted the mean and divided by the standard deviation. This gives us a new variable (standardized fluorescence intensity for each pore) with mean of 0 and standard deviation of 1. We now combine the series into a single data set that should follow a normal distribution if the distribution of the original observations are a multiple of the Poisson distribution. The combined data are shown as a histogram, and the line represents the normal distribution.

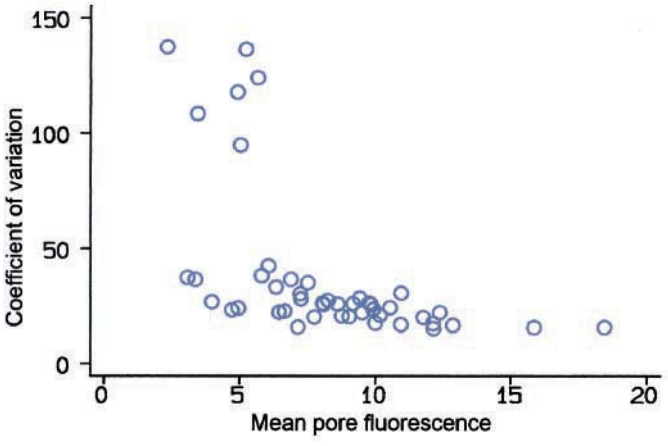

FIGURE 7 Variability of fluorescence intensity of individual PET pores exposed to DiO-C_2-(3). We calculated the coefficient of variation (mean/standard deviation) for 30 successive determinations of fluorescence intensity (see, for example, Fig. 5, *a–c*) of each of 46 different pores. Data are presented as coefficient of variation versus mean fluorescence intensity.

cence intensity in the 46 pores that we investigated to see whether the changes of intensity fluctuate together. Because fluorescence intensity is proportional to the number of dye molecules in the image slice selected by the confocal microscope we might expect that time variations in intensity would follow a Poisson distribution. To compare the distributions of all the pores it is necessary to transform each of them into a form where this can be done simply. For Poisson distributions this can be achieved by taking the square root of the original values for each pore, finding the mean and standard deviation for each pore and then subtracting the mean from each data point and dividing by the standard deviation. The transformed data for each pore have a mean of zero and a standard deviation of one. The distribution of all the data points, thus transformed (Fig. 6) is very close to a normal distribution. This is consistent with data for each pore following a Poisson distribution multiplied by a constant (the efficiency of sampling in each case). We have also calculated the coefficient of variation (mean/standard deviation) for the raw data for each of the 46 pores. If we plot coefficient of variation against mean fluorescence intensity (Fig. 7) we find two classes of pore (presumably as a result of the tracking and etching processes). The majority (40/46) have a coefficient of variation of 25% irrespective of the mean intensity. The remainder (6/46) have low mean intensity but very high coefficients of variation, greater than 100%. These pores (13%) probably correspond to those that by electrophysiological techniques show substantial fluctuations of ion current; in our experience, the fraction of pores on any one day that do this is ~10%. Since the two populations of pores come from different pieces of PET, we assume that the high coefficient of variation arises because of the nature of particular pores and not because of the limitations of the detection system.

It could be argued that fluctuations of fluorescence of compounds like diO-C_2-(3) and fluorescein, which are partly hydrophobic, are a consequence of changes in hydrophobicity of the membrane surface. Because protonated carboxyl groups are more hydrophobic than ionized carboxyl groups, the consequence of this interpretation is the same as that given above, and we would not quarrel with such a view. It could, furthermore, be maintained that fluctuations of dye binding, as well as of ionic current, are due not so much due to changes in ionization as to changes in architecture of the membrane between an open and a closed configuration. We have argued elsewhere (Korchev et al., 1997; Rostovtseva et al., 1996) against such an interpretation. Instead, we propose that our experiments show, for the first time to the best of our knowledge, that the ionization of fixed charges in a confined space, such as a narrow pore or the space between two closely apposed surfaces, oscillates at a time scale many orders of magnitude slower than that anticipated from the on and off rate of protons in free solution. The reasons for such an enormous decrease are a consequence of the ionic interactions between fixed charges that are separated by no more than a few angstroms (Manning, 1969; Korchev et al., 1997).

Our model of a fluctuating surface charge is largely dismissed by Hille (1992) for biological ion channels on the grounds that in the one instance where permeation of uncharged molecules has been measured, the changes that affect ion current also affect permeability. In PET pores the opposite situation holds, namely, that permeability of uncharged molecules is unaffected by surface charge (Rostovtseva et al., 1996). The model is therefore unlikely to provide the major explanation for the fluctuation of ion conductance in endogenous ion channels. But in those instances where fixed charges may contribute to an anomalously high conductance despite high selectivity, as in Ca^{2+}-activated K^+ maxi channels (Laver and Gage, 1997), it is possible that fluctuations of surface charge underlie the fluctuations of ion current that are observed. Moreover, the oscillations in ion channels described as open-channel noise (Sigworth, 1985; Heinemann and Sigworth, 1991), which also occur in toxin-induced channels (Bezrukov and Kasianowicz, 1993), may be partly due to fluctuations of surface charge. Although they occur much more rapidly than the fluctuations in PET pores, the difference in timescale is approximately of the same order as the difference in length, around 1000-fold, and may reflect the timescale of conformational/configurational changes of very differing space dimension. In those toxin-induced pores in which the low-conductance state has been shown to be still permeable to organic solutes (Korchev et al., 1995), fluctuations of surface charge do appear to account for the observed oscillations in ion current (Korchev et al., 1997). This interpretation is likely to apply especially to pores that show oscillations of conductance yet whose effective diameter is 10 nm or greater; pores induced by toxins such as *Clostridium perfringens* θ toxin (Menestrina et al., 1990) and immune molecules such as activated complement (Bhakdi and Tranum-Jensen, 1984) or the cytolysin from cytotoxic T cells (Henkart, 1985) are examples. Finally, as nanopore technology (Bashford, 1999; Rao et al., 1999) becomes applied to the fabrication of ion channel devices, the behavior of fixed charges in a confined space that we have described will need to be taken into account. Indeed it may lead to quite novel applications in situations where normal transmission of nerve impulses fails.

We are grateful to Dr. Reimar Spohr and Dr. P. Y. Apel for the gift of track-etched membranes and to Drs. Martin Bland, Donald Edmonds, Apolinario Nazarea, and Terry Poulton for much helpful advice.

This work was supported by the Biotechnology and Biological Sciences Research Council and the Cell Surface Research Fund.

REFERENCES

Bashford, C. L. 1999. Model membranes. *In* Biosciences 2000: Current Aspects and Prospects for the Next Millennium. C. A. Pasternak, editor. Imperial College Press, London. 233–245.

Bashford, C. L., and C. A. Pasternak. 2000. Membrane pores. *In* Advances in Structural Biology, Vol. 6. S. K. Malhotra, editor. JAI Press, Stamford, CT. 303–326.

Bezrukov, S. M., and J. J. Kasianowicz. Current noise reveals protonation kinetics and number of ionizable sites in an open protein ion channel. 1993. *Phys. Rev. Lett.* 70:2352–2355.

Bhakdi, S., and J. Tranum-Jensen. 1984. Mechanism of complement cytolysis and the concept of channel-forming proteins. *Phil. Trans. Roy. Soc. Lond. B.* 306:311–324.

Bhushan, B., J. N. Israelachvili, and U. Landman. 1995. Nanotribology: friction, wear and lubrication at the atomic-scale. *Nature.* 374: 607–616.

Bland, J. M. 2000. An Introduction to Medical Statistics, 3rd ed. Oxford University Press, Oxford, UK.

Granick, S. 1991. Motions and relaxations of confined liquids. *Science.* 253:1374–1379.

Heinemann, S. H., and F. J. Sigworth. 1991. Open channel noise. VI. Analysis of amplitude histograms to determine rapid kinetic parameters. *Biophys. J.* 60:577–587.

Henkart, P. A. Mechanism of lymphocyte-mediated cytotoxicity. 1985. *Annu. Rev. Immunol.* 3:31–58.

Hille, B. 1992. Ionic Channels of Excitable Membranes. Sinauer, Sunderland, MA. 295–298, 479.

Korchev, Y. E., C. L. Bashford, G. M. Alder, J. J. Kasianowicz, and C. A. Pasternak. 1995. Low conductance states of a single ion channel are not 'closed'. *J. Membr. Biol.* 147:233–239.

Korchev, Y. E., C. L. Bashford, G. M. Alder, P. Y. Apel, D. T. Edmonds, A. A. Lev, K. Nandi, A. V. Zima, and C. A. Pasternak. 1997. A novel explanation for fluctuations of ion current through narrow pores. *FASEB J.* 11:600–608.

Lakshminarayanaiah, N. 1969. Transport Phenomena in Membranes. Academic Press, New York.

Laver, D. R., and P. W. Gage. 1997. Interpretation of substates in ion channels: unipores or multipores? *Prog. Biophys. Mol. Biol.* 67: 99–140.

Lev, A. A., Y. E. Korchev, T. K. Rostovtseva, C. L. Bashford, D. T. Edmonds, and C. A. Pasternak. 1993. Rapid switching of ion current in narrow pores: implications for biological ion channels. *Proc. R. Soc. Lond. B.* 252:187–192.

Manning, G. S.1969. Limiting laws and counterion condensation in polyelectrolyte solutions. I. Colligative properties. *J. Chem. Phys.* 51: 924–933.

Menestrina, G., C. L. Bashford, and C. A. Pasternak. 1990. Pore-forming toxins: experiments with *S. aureus* alpha-toxin, *C. perfringens* theta-toxin and *E. coli* haemolysin in lipid bilayers, liposomes and intact cells. *Toxicon.* 28:477–491.

Pasternak, C. A., G. M. Alder, P. Y. Apel, C. L. Bashford, D. T. Edmonds, Y. E. Korchev, A. A. Lev, G. Lowe, M. Milovanovic, C. W. Pitt, T. K. Rostovtseva, and N. I. Zhitarivk. 1995. Nuclear track-etched filters as model pores for biological-membranes. *Radiat. Measure.* 25:675–683.

Rao, C. N. R., R. Sen, B. C. Satishkumar, and A. Govindaraj. 1999. Nanotubes of carbon and other materials. *In* Biosciences 2000: Current Aspects and Prospects for the Next Millennium. C. A. Pasternak, editor. Imperial College Press, London. 247–275.

Raviv, U., P. Laurat, and J. Klein. 2001. Fluidity of water confined to subnanometre films. *Nature.* 413:51–54.

Rostovtseva, T. K., C. L. Bashford, G. M. Alder, G. N. Hill, C. McGiffert, P. Y. Apel, G. Lowe, and C. A. Pasternak. 1996. Diffusion through narrow pores: movement of ions, water and nonelectrolytes through track-etched PETP membranes. *J. Membr. Biol.* 151:29–43.

Sachs, F., and F. Qin. 1993. Gated ion selective channels observed with patch pipettes in the absence of membranes: novel properties of a gigaseal. *Biophys. J.* 65:1101–1107.

Schwartz, G. A. 1962. Theory of the low-frequency dielectric dispersion of colloidal particles in electrolyte solution. *J. Phys. Chem.* 66:2636–2642.

Sigworth, F. J. 1985. Open channel noise. I. Noise in acetylcholine-receptor currents suggests conformational fluctuations. *Biophys. J.* 47: 709–720.

Sims, P. J., A. S. Waggoner, C. H. Wang, and J. F. Hoffman. 1974. Studies on the mechanism by which cyanine dyes measure membrane potential in red blood cells and phosphatidylcholine vesicles. *Biochemistry.* 13: 3315–3330.

Spitzer, J. J. 1984. A re-interpretation of hydration forces near charged surfaces. *Nature.* 310:396–397.

Spohr, R. 1990. Ion Tracks and Microtechnology. F. Vieweg and Sons, Braunschweig, Germany.

Wolf, A., N. Reber, P. Y. Apel, and R. Spohr. 1995. GSI Nachrichten.